View metadata, citation and similar papers at core.ac.uk
brought to you by CORE
provided by UT Digital Repository

MODELING THE FRACTURE STRENGTH BETWEEN FUSED-DEPOSITION EXTRUDED ROADS

J. P. Thomas† and J. F. Rodríguez*

† NOVA Research Inc., Naval Research Laboratory, Code 6350, Washington, DC 20375
* Department of Mechanics, University of Simon Bolivar, Caracas, Venezuela

Abstract

The fracture strength developed between Fused-Deposition extruded roads is modeled in terms of the wetting and thermally-driven diffusion bonding processes. Thermal histories at the road-to-road interface are obtained from a heat transfer analysis and used to develop model predictions based on reptation theory for the interdiffusion of long-chain polymer molecules. Fracture toughness data on FD-ABS plastic specimens is used to quantify the model. The results show that most of the fracture strength develops during the surface wetting stage of bonding and that slower cooling rates during solidification promote stronger bonding between the roads.

Introduction

Fused-Deposition (FD) creates a physical representation of a CAD model via computer-controlled robotic extrusion of a small polymeric "road" or "fiber" in a layer-by-layer additive material deposition process (Figure 1). The roads are extruded in a semi-liquid state and bond with the neighboring roads by molecular interpenetration at the interfaces to form the solid model. The strength of the bonds directly affects the mechanical strength of the FD model. The flexibility of the FD process to create geometrically complex parts with tailored mesostructural characteristics (i.e., features at the scale of the extruded fiber diameter $\sim 0.1\,mm$) endow it with unique potential for the manufacture of multifunctional materials and parts with optimized performance. However, a better understanding of the effect of the FD variables like extrusion and envelope temperatures and road dimensions on the bonding process is needed before this potential can be exploited.

We describe herein the results of a combined analytical-computational-experimental study of the fiber-to-fiber interface strength of FD-ABS plastic materials. Previous studies pertaining to FD-ABS mesostructure, stiffness, and strength are reported in [1-4]. After presenting some background on thermally-driven molecular bonding between like polymers, a description of the analytical/computational methods used to model the bond strength as a function of various parameter values is given. Experimental fracture toughness measurements are used quantify the model. The model is then used to make interface toughness estimates for process variable settings of possible interest. The results show that most of the fracture strength develops during the surface wetting stage of bonding and that slower cooling rates during solidification promote stronger bonding between the roads.

Background

The bonding of similar polymers involves a process of interpenetration of the molecular chains across an interface. The process is thermally activated and only occurs at temperatures above the polymer's glass transition temperature. As molecular interpenetration increases, the interface gradually disappears and mechanical strength develops. Wool and O'Connor [5] model

the bonding process using reptation theory, a special type of mass diffusion that occurs in five stages: (i) surface rearrangement, (ii) surface approach, (iii) wetting, (iv) diffusion, and (v) randomization. Surface rearrangement and approach occur prior to surface contact. During wetting, barriers to molecular interpenetration related to inhomogeneities on the interface disappear, and by the end of this stage, the chains are free to move across the interface via reptation diffusion.

A macroscopic recovery function (normalized fracture toughness), $R(t)$, is defined for ***isothermal*** conditions in terms of the convolution between an intrinsic healing function for wetting and diffusion, $R_h(t)$, and a wetting distribution function, $\phi(t)$ [5]:

$$R(t) = \int_0^t R_h(t-\tau)\frac{d\phi(t)}{dt}d\tau = \frac{K(t)}{K_\infty} \tag{1}$$

where $K(t)$ is the interface toughness after time t at some constant temperature T, and K_∞ is the fracture toughness of the virgin material. The convolution integral represents bonding as the sum of wetting and diffusion processes initiated at different times. The intrinsic healing function $R_h(t)$ is given by:

$$R_h(t) = R_0 + (1-R_0)\left(\frac{t}{t_\infty(T)}\right)^{\frac{1}{4}} \tag{2}$$

where R_0 is the normalized toughness that develops on wetting and $t_\infty(T)$ is the reptation time as a function of temperature, T. Note that $R_h(t_\infty) = 1$, signifying full recovery of the interface toughness to the "virgin" material value.

The temperature dependence of t_∞ can be modeled using the WLF equation [6]:

$$log\left(\frac{t_\infty(T)}{t_\infty(T_s)}\right) = -\frac{8.86\,(T-T_s)}{101.6+T-T_s} \tag{3}$$

with t_∞ in $min.$ and T in $°K$. Values for T_s and $t_\infty(T_s)$ are determined from interface toughness data from annealed FD-ABS specimens. The wetting distribution function is taken as:

$$\phi(t) = \phi_0 + (1-\phi_0)\left(1-e^{-kt^m}\right) \tag{4}$$

where ϕ_0 is the instantaneous fractional gain of wetted area at $t=0$, and $(1-e^{-kt^m})$ is a generalized Avrami-Erofeev reaction kinetics model [7] characterizing the nucleation and growth of wetted area at the interface. k is a thermally-activated rate constant, and m characterizes the order of the reaction. We have assumed that k is constant and consider values of $m = 1, 2,$ and 3 corresponding to: diffusion controlled growth of the wetted area with instantaneous nucleation, linear growth with instantaneous nucleation or diffusion controlled growth with linear nucleation, and linear growth with linear nucleation, respectively [5].

Equation (1) can be integrated to give:

$$R(t) = \phi_0 R_h(t) + R_0(1-\phi_0)\left(1-e^{-kt^m}\right) + I_m \tag{5}$$

where $R_h(t)$ is given by Eq. (2), and I_m is given by:

$$I_m = km(1-\phi_0)(1-R_0)\,B\left(\frac{5}{4}, m\right)\frac{t^{m+\frac{1}{4}}}{t_\infty^{1/4}} \times \tag{6}$$

$$\times\ {}_mF_m\left(1, \frac{m+1}{m}, \cdots, \frac{2m-1}{m};\ \frac{5/4+m}{m}, \frac{9/4+m}{m}, \cdots, \frac{5/4+2m-1}{m};\ -kt^m\right)$$

$B\left(\frac{5}{4}, m\right)$ is the Beta function, and ${}_mF_m\left(1, \frac{m+1}{m}, \cdots;\ \frac{5/4+m}{m}, \frac{9/4+m}{m}, \cdots;\ -kt^m\right)$ is the generalized hypergeometric series.

Bastien and Gillespie [8] numerically extended a similar polymer healing model to nonisothermal conditions by dividing the thermal history into small, constant-temperature time intervals, and then summing to obtain $R(t)$. In an analogous fashion, we have extended the model to nonisothermal conditions by implicitly differentiating Eq. (5) with respect to time and then integrating over the temperature history. That is:

$$R(t_g) = R_0(1-\phi_0)\left(1-e^{-kt_g^m}\right) + \phi_0\int_0^{t_g}\frac{\partial R_h(\tau)}{\partial\tau}d\tau + \int_0^{t_g}\frac{\partial I_m(\tau)}{\partial\tau}d\tau \tag{7}$$

where t_g is the time it takes for the FD interface to cool to the glass transition temperature, T_g, and t_∞ is taken as $t_\infty(T(\tau))$ during the integration. The first term can be written explicitly because it does not depend on temperature (i.e., t_∞). Eq. (7) is the analytical (infinitesimal) version of Bastien and Gillespie's extension and evaluates to the standard isothermal expression when T is constant.

Method

Application of Eq. (7) to the fiber-to-fiber interface bonding process during FD requires selection of a reaction order value: m, estimates for the model parameters: R_0, ϕ_0, k and WLF parameters: T_s and $t_\infty(T_s)$, and the interface temperature history, $T(t)$, during FD fabrication. We determine values for K_∞, R_0, ϕ_0, k, T_s, and $t_\infty(T_s)$ for $m = 1, 2,$ and 3 using experimental interface fracture toughness values from FD-ABS specimens fabricated at various extrusion and envelope temperatures, T_L and T_E, with and without post fabrication annealing treatment. The interface temperature histories are obtained using an analytical heat transfer analysis of the FD process. These temperature histories are integrated in Eq. (7) and the results used in a nonlinear regression analysis to obtain the model parameter estimates. Interface toughness predictions for any FD process are then possible given the interface temperature history.

A 2-D transient heat transfer analysis of a single-road-width FD solidification process is performed. The analysis is simplified by assuming the roads are rectangular in shape and vertically stacked with four fibers forming the base (Figure 2). The road width, W, is taken to be $0.504\,mm$, and the road height, H, $0.254\,mm$. The governing equation, expressed using the normalized temperature $T^* = (T - T_E)/T_E$, is given by:

$$\frac{\partial^2 T^*}{\partial x^2} + \frac{\partial^2 T^*}{\partial y^2} = \frac{1}{\alpha^2}\frac{\partial T^*}{\partial t} \tag{8}$$

with boundary and initial conditions:

$$\begin{array}{lll} \frac{\partial T^*(-W/2,y,t)}{\partial x} = \frac{h}{k}T^* & \frac{\partial T^*(x,5H,t)}{\partial y} = -\frac{h}{k}T^* & \frac{\partial T^*(W/2,y,t)}{\partial x} = -\frac{h}{k}T^* \\ T^*(x, 4H \le y \le 5H, 0) = T_L^* & T^*(x, 0 \le y \le 4H, 0) = 0 & \end{array} \tag{9}$$

The eigenfunction expansion solution, averaged over the width, is given by:

$$T_{ave}(x,y,t) = T_E + \frac{2T_E}{W}\sum_{m=1}^{\infty}\sum_{n=1}^{\infty}\left(\frac{a_{mn}}{\beta_n}\, sin(\lambda_m y)\, cos\left(\frac{\beta_n W}{2}\right)\right) e^{-\alpha^2(\lambda_m^2+\beta_n^2)t} \tag{10}$$

where the various terms are defined in the Appendix. Material properties taken for the ABS are: $k = 0.177\frac{W}{m\,K}$; $C_p = 2080\,\frac{J}{kg\,K}$; $\rho = 1050\,\frac{kg}{m^3}$, and a convection coefficient: $h = 30\,\frac{W}{m^2\,K}$ based on natural convection from a flat horizontal plate. Numerical values are computed in Maple using 15-digit calculations. The algorithm and calculations are verified by comparing with an independent 1-D transient solution obtained using Laplace transforms.

The influence of the number of base fibers in the stack, $N = 1,\ 2,\ 4$, and 10; the convection coefficient, $h = 5$, 30, and 100; and the number of terms needed in the expansion, m & $n = 10$, 50, 100, and 250 have all been determined. Essentially identical interface temperature histories are obtained for $N \ge 2$. Slightly longer cooling times occur as h decreases, and the difference between the center ($x = 0$) and edge ($x = \pm W/2$) temperatures increases as h increases. Accuracy of the interface temperature at short times $t \sim 10^{-4}\,sec$ requires m & $n \ge 100$ in the solution expansion due to the oscillatory Gibbs effect. While this may seem large (100^2 terms in the expansion), the computations are quick and accurate in Maple.

A Stratasys FDM1600 was used to make fracture specimens out of P400 acrylonitrile-butadiene-styrene (ABS) plastic. Single-edge-notch fracture specimens were made from single-fiber width ($0.508\,mm$ nominal thickness) square cylinders $50.8 \times 50.8 \times 58.4\,mm$ fabricated at the processing temperatures shown in Table 1. A number of specimens made with $T_L = 270°C$ and $T_E = 70°C$ were annealed at 118, 125, and $134\ \pm 1°C$ from $1\,minute$ to $8\,hours$ to obtain data for the WLF parameters. Details of the experiments can be found in references [3,4].

Extrusion Temperature, $T_L\,[°C]$	255	270	285
Envelope Temperatures, $T_E\,[°C]$	50, 60, 70	50, 60, 70	50, 60, 70

Table 1: FD processing temperature used in the experimental interface fracture study.

The fracture toughness tests on the annealed specimens were used to determine T_s and $t_\infty(T_s)$ in the WLF relationship. The data start from $K_0 = 1.88\,MPa\sqrt{m}$ corresponding to FD fabrication at $T_L = 270°C$ and $T_E = 70°C$. In Figure 3, it can be seen that the toughness levels-out to $2.47\,MPa\sqrt{m}$ for the $134°C$ anneal; this value is taken as K_∞, the virgin P400 ABS material toughness. The toughness increases during annealing according to the $t^{1/4}$ relationship:

$$\frac{K - K_o}{K_\infty} = \left(\frac{t}{t_\infty}\right)^{1/4} \tag{11}$$

The WLF parameter estimates are obtained by fitting a straight lines to the data in Figure 3, then extrapolating out-in-time to $(K - K_0)/K_0 = 1$ where $t = t_\infty$ for that particular anneal

temperature. A nonlinear regression analysis using the three t_∞ values provides estimates for T_s and $t_\infty(T_s)$.

The temperature-time related terms in Eq. (7) are numerically integrated in double-precision Fortran after least-squares fitting the interface temperature histories (T -vs.- t) with cubic splines. Series representations for the generalized hypergeometric functions are used in the integration routine. The number of terms needed for accurate representation of ${}_mF_m$ depends on the values of m and k. Fifteen terms provides an accuracy of 1% for k values less than: 0.7 ($m = 1$), 9.7 ($m = 2$), and 16 ($m = 3$) for $t = 8.3\,sec$ (largest t_g value).

Estimates for R_0, ϕ_0, and k for $m = 1$, 2, and 3 were obtained by nonlinear regression of the interface fracture data (dependent variable) against the RHS of Eq. (7) using a Marquardt-Levenberg algorithm in the PC program SigmaPlot.

Results

Figure 4 shows the width-averaged interface temperature histories for a variety of FD processing conditions. Cooling to the glass transition temperature takes from 1.74 to 15.9 $seconds$ for the half and double-sized FD roads respectively. The most influential factor in the cooling process appears to be the road cross-sectional area.

Figure 3 shows that the interface toughness values for the annealed specimens behave according to the $t^{1/4}$ relationship of Eq. (11). Figure 5 shows a scatter plot of t_∞ values obtained from the data in Figure 3 and the corresponding WLF relationship (Eq. (3)). The estimate for T_s, $143°C = T_g + \ 49°C$, agrees very well with value recommended in reference [6].

Table 2, below, summarizes the results of the nonlinear fitting of Eq. (7) to the experimental interface toughness values. "All Data" refers to fitting using K values for specimens fabricated at $T_L = 255$, 270, and $285°C$ with $T_E = 50$, 60, and $70°C$, while "$270\,\&\,285°C$" refers to fitting of K values for specimens fabricated at $T_L = 270$ and $285°C$ with $T_E = 50$, 60, and $70°C$.

	All Data			**$270\,\&\,285°C$**		
$\boldsymbol{m}$	**1**	**2**	**3**	**1**	**2**	**3**
$\boldsymbol{\phi_0}$	0.143	0.551	0.685	0.426	0.608	0.764
$\boldsymbol{\sigma_{\phi_0}}$	1.395	0.304	0.150	0.023	0.073	0.022
$\boldsymbol{R_0}$	0.807	0.724	0.697	1.000	0.950	0.756
$\boldsymbol{\sigma_{R_0}}$	0.329	0.111	0.069	0.122	0.147	0.040
$\boldsymbol{k\,[1/sec]}$	0.357	0.075	0.016	0.149	0.019	0.008
$\boldsymbol{\sigma_k}$	0.837	0.106	0.019	0.050	0.009	0.004
$\boldsymbol{R_{reg}}$	0.8082	0.8211	0.8237	0.9986	0.9962	0.9926
$\boldsymbol{\sigma_{reg}}$	0.0562	0.0545	0.0541	0.0035	0.0057	0.0079

Table 2: Nonlinear regression results. The σ quantities are standard error estimates. The $270\,\&\,285°C$/ $m = 3$ parameter values are used to make the K predictions in Figure 6.

Figure 6 shows a scatter plot of the predicted and experimental interface toughness values. The predictions (solid and hollow symbols) are made using the ϕ_0, R_0, and k values obtained from the "$270\,\&\,285°C$" data and $m = 3$. The x's on the curves correspond to the measured values. Note the discrepancy between the predicted and experimental toughness values at $T_L = 255°C$.

Discussion

The analytical heat transfer model provides a quick and useful method for investigating the influence of various FD processing conditions on the interface temperature history. However, limitations and approximations of the model should kept in mind. First, the model does not account for heat transfer along the fiber axis. The nozzle speed during extrusion is an important factor in this respect. The 2-D model will be more accurate as the extrusion rate increases because of the expected decrease in temperature gradient along the fiber axis. The assumed road geometry (rectangular), and the value selected for the convection coefficient, h, also play an important role in the accuracy of the calculated temperature histories. Numerical modeling (e.g., finite elements) could be used to examine more realistic road geometries, but the problem of correctly modeling the convective heat transfer conditions along the sides and top of the road (i.e., specification of h) remains. Fortunately, the influence of h on the temperature history is not too large for the values of interest. Application to multiple-road-width parts would require consideration of a new heat transfer problem with a conduction boundary condition on one side of the fiber. This can easily be accomplished and will be examined in the future.

Table 2 shows that the bonding model fits the $T_L = 270$ & $285°C$ data much better (e.g., $R_{reg} \sim 0.99$-vs.-0.82). This, plus the nonrandom nature of the residuals ($K_{pred} - K_{exp}$), likely indicates the need to include a temperature dependence in the rate constant, k, of the form:

$$k = k_0 \, exp\left(\frac{-A(T)}{RT} \right) \tag{12}$$

One could assume that the activation energy, A, is a constant (i.e., a standard Arrhenius model), or allow A to be temperature dependent. If A is constant or if its temperature dependence follows the same WLF relation as the anneal data, then only one parameter is added to the regression model. If the temperature dependence of A is otherwise unspecified, then the analysis is greately complicated because of the temperature-time integration.

Another possibility for the lack of fit at $T_L = 255°C$ is a temperature dependent change in microstructure that influences the bond strength. For example, coalescence and growth of the butadiene rubber particle size at the higher extrusion temperatures would presumably lead to lower bond strengths. This possibility is currently being explored by micrographic examination of FD-ABS material extruded at various extrusion and envelope temperatures.

The selection of an appropriate m value (1, 2, or 3) is not possible with the present data. The $m = 2$ and 3 models seem to provide more reasonable R_0 and ϕ_0 values than $m = 1$. The extent of wetting (i.e., $\phi(t_g)$) varies from 0.63 ($T_L = 255$ and $T_E = 50°C$) to 0.77 ($T_L = 285$ and $T_E = 70°C$) for $m = 1$ to approximately 1.0 for all extrusion and envelope temperatures with $m = 2$ and 3. Fractography of the toughness specimens does not show any visible signs of voids in the surface. Fortunately, these models ($m = 1$, 2, and 3) exhibit large differences in their toughness predictions for different sized specimens. Comparison between the predicted and experimental values can be used as a definitive test of the different models.

Closure

A wetting-diffusion model for FD-ABS bonding has been presented. A number of issues regarding the approximations made in applying the model, appropriate parameter functional forms, and determination of the parameter values have been raised. The ability of the model to predict interface toughness values requires further investigation but promises to be very useful in

guiding the selection of FD processing parameter values for maximizing strength and in the development of mechanistic FD material strength models.

In qualitative terms, the model shows that factors which prolong the fiber solidification times lead to increases in the bonding strength. Doubling the road size had the largest effect, increasing the bond strength to that of the virgin ABS material. Post fabrication annealing also increases the bond strength, but specimen warping due to the relaxation of residual stresses would have to be addressed. Raising the envelope temperature to $80°C$ increases the predicted bond strength by $\sim 5\%$. This is not possible with the FDM1600, but current Stratasys hardware does allow for higher envelope temperatures.

References

1. J. F. Rodríguez, J. P. Thomas, J. E. Renaud, 2000, *Rapid Prototyping Journal*, to appear.
2. J. F. Rodríguez, J. P. Thomas, J. E. Renaud, 2000, Paper No. DAC-14296 in *ASME Proc. of DETC'00*, pp. 1-8.
3. J. F. Rodríguez, J. P. Thomas, J. E. Renaud, 1999, in *Proc. 10th SFF Symposium*, Austin, TX, pp. 335-342.
4. J. F. Rodríguez, J. P. Thomas, J. E. Renaud, 1999, in *Proc. SME RP&M Conf.*, pp. 629-643.
5. R. P. Wool, K. M. O'Connor, 1981, *Journal of Applied Physics*, **52**, pp. 5953-5963.
6. M. L. Williams, R. F. Landel, J. D. Ferry, 1955, *J. Amer. Chem. Soc.*, **77**, pp. 3701-3707.
7. J. E. House, 1997, *Principles of Chemical Kinetics*, W. C. Brown Pub., Dubuque, IA.
8. L. J. Bastien, J. W. Gillespie, 1991, *Poly. Engr. & Sci.*, **31**, pp. 1720-1730.

Appendix

$$a_{mn} = \frac{4T_L^*}{E_m^2\, F_n^2\, \lambda_m\, \beta_n}\, sin\left(\frac{9\lambda_m H}{2}\right) sin\left(\frac{\lambda_m H}{2}\right) sin\left(\frac{\beta_n W}{2}\right)$$

$$E_m^2 = \frac{1}{2}\left(5H - \frac{sin(10\lambda_m H)}{2\lambda_m}\right) \quad \text{and} \quad F_n^2 = \frac{1}{2}\left(W + \frac{sin(\beta_n W)}{\beta_n}\right)$$

λ_m and β_n from solving: $\quad \lambda_m\, cot(5\lambda_m H) = \frac{-h}{k} \quad$ and $\quad \beta_n\, tan\left(\frac{\beta_n W}{2}\right) = \frac{h}{k}$

$$\alpha^2 = \frac{k}{C_p\, \rho}$$

Figures

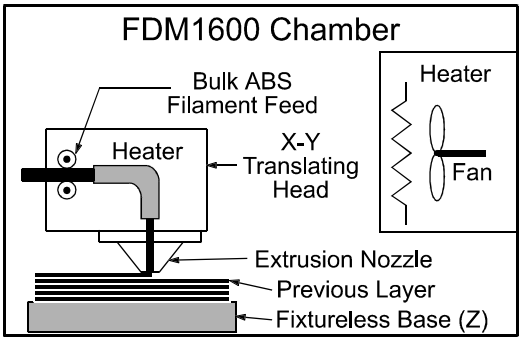

Figure 1: Schematic of the Fused-Deposition hardware and fiber "road" extrusion process.

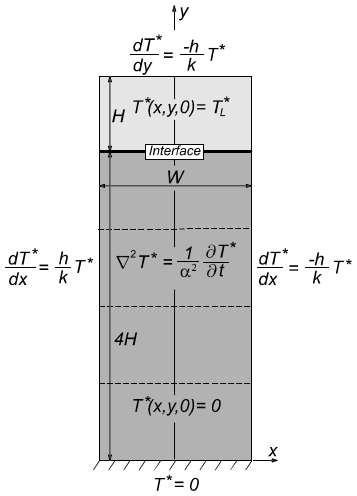

Figure 2: Single-road FD heat-transfer model.

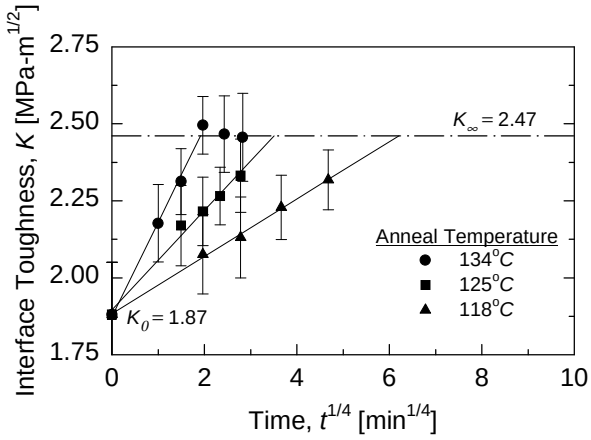

Figure 3: Interface fracture toughness for the annealed specimens showing a $t^{1/4}$ dependence.

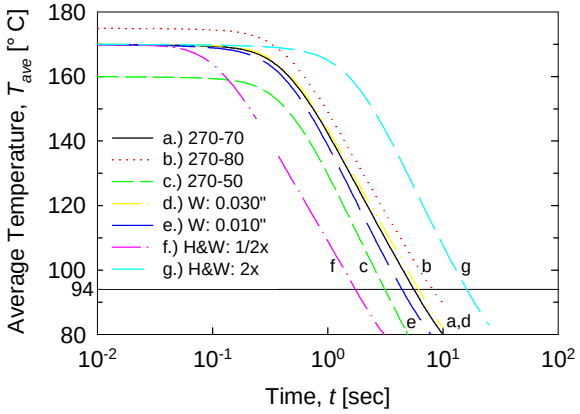

Figure 4: Temperature histories for a number of FD processing conditions.

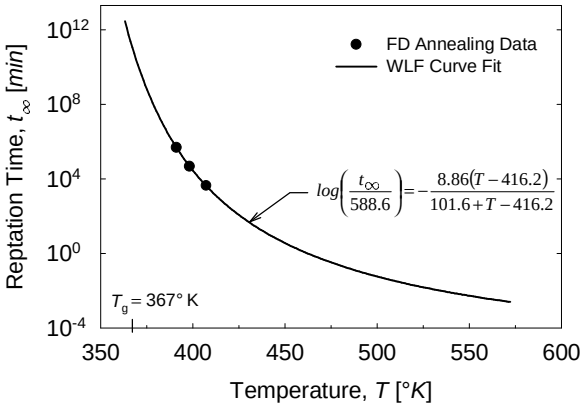

Figure 5: WLF scatter plot showing the temperature dependence of t_∞.

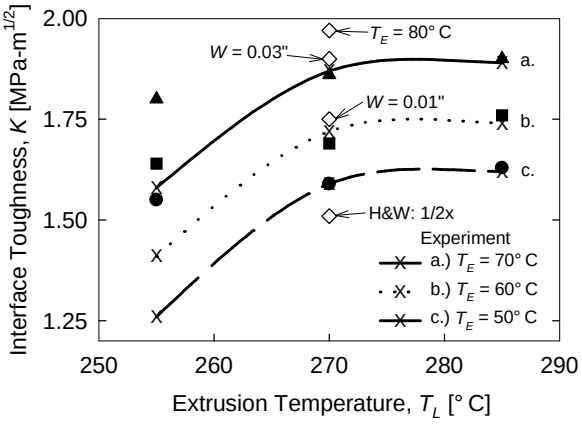

Figure 6: Experimental and predicted interface toughness values. The predicted toughness for H&W: 2x is not shown on the plot, but equals 2.47 $MPa\sqrt{m}$.